

Optimization of Binary Thermodynamic and Phase Diagram Data

CHRISTOPHER W. BALE and A. D. PELTON

An optimization technique based upon least squares regression is presented to permit the simultaneous analysis of diverse experimental binary thermodynamic and phase diagram data. Coefficients of polynomial expansions for the enthalpy and excess entropy of binary solutions are obtained which can subsequently be used to calculate the thermodynamic properties or the phase diagram. In an interactive computer-assisted analysis employing this technique, one can critically analyze a large number of diverse data in a binary system rapidly, in a manner which is fully self-consistent thermodynamically. Examples of applications to the Bi-Zn, Cd-Pb, PbCl₂-KCl, LiCl-FeCl₂, and Au-Ni binary systems are given.

I. INTRODUCTION

FOR a binary solution phase, many diverse sets of experimental thermodynamic data may be available. Activities of one or more components at various compositions and temperatures may have been measured by emf, vapor pressure, mass spectrometric, or other techniques. Enthalpies of mixing may have been determined calorimetrically. The experimental equilibrium phase diagram is also a source of thermodynamic data. If the Gibbs energy of fusion of a stoichiometric component is known, for example, then the activity of this component in the liquid phase can be calculated (nonisothermally) along its liquidus. Even a miscibility gap is a source of thermodynamic data, since the activity of either component is the same at both ends of any tie-line, even though the actual values of the activities may not be known.

The various thermodynamic properties are all related via the Gibbs-Helmholtz and Gibbs-Duhem equations. If sufficient data are available, then in principle it is possible to obtain one "optimum" equation for the Gibbs energy of the solution as a function of temperature and composition. Obtaining such an expression involves the critical assessment and correlation of all the data as well as the testing of the data for internal consistency. In practice, however, such an operation is not an easy task due to the complexity of the relationships among the various measured properties.

The development and application of techniques to perform such analyses is a subject of current interest.¹⁻⁶ In the present article, a linear least squares optimization technique is proposed which can be used in a computer-assisted critical analysis of binary thermodynamic and phase diagram data including liquidus/solidus lines of components and intermediate compounds as well as miscibility gap boundaries.

For a binary solution of components A and B, the integral molar Gibbs energy of mixing relative to the pure components is expressed as:

$$\Delta g = RT(X_A \ln X_A + X_B \ln X_B) + g^E \quad [1]$$

where X_A , X_B are the mole fractions and g^E is the excess integral molar Gibbs energy. (For certain systems, a dif-

ferent choice of the ideal terms in Eq. [1] may be more convenient.) g^E may be expressed as a polynomial in the mole fraction X_A :

$$g^E = \sum_{j=1}^M \phi_{m_j n_j} X_A^{m_j} (1 - X_A)^{n_j} \quad [2]$$

where the $\phi_{m_j n_j}$ are coefficients, M is the total number of such coefficients, and m_j and n_j are positive integral powers. For example, in a regular solution, $M = 1$, $m_1 = n_1 = 1$, and g^E is quadratic:

$$g^E = \phi_{11} X_A (1 - X_A) \quad [3]$$

In a "sub-regular" solution, $M = 2$, and g^E is cubic:

$$g^E = \phi_{11} X_A (1 - X_A) + \phi_{12} X_A (1 - X_A)^2 \quad [4]$$

There is some freedom in how the two terms of a sub-regular solution expression may be chosen. For example, one could have written Eq. [4] in terms of ϕ_{11} and ϕ_{21} , or in terms of ϕ_{12} and ϕ_{21} . All these cubic expressions would be equivalent.

The coefficients $\phi_{m_j n_j}$ may be written as linear functions of temperature, T :

$$\phi_{m_j n_j} = h_{m_j n_j} - T s_{m_j n_j} \quad [5]$$

Hence, the integral molar enthalpy of mixing and excess entropy of mixing, assumed independent of T , are given in terms of the coefficients $h_{m_j n_j}$ and $s_{m_j n_j}$ as:

$$\Delta h = \sum_{j=1}^M h_{m_j n_j} X_A^{m_j} (1 - X_A)^{n_j} \quad [6]$$

$$s^E = \sum_{j=1}^M s_{m_j n_j} X_A^{m_j} (1 - X_A)^{n_j} \quad [7]$$

The partial excess Gibbs energy of A, g_A^E , may be obtained from differentiation of Eq. [2] via the expression:

$$g_A^E = g^E + (1 - X_A) \frac{dg^E}{dX_A} \quad [8]$$

to give:⁷

$$g_A^E = \sum_{j=1}^M \phi_{m_j n_j} [m_j X_A^{m_j-1} + (1 - m_j - n_j) X_A^{m_j}] (1 - X_A)^{n_j} \quad [9]$$

CHRISTOPHER W. BALE, Associate Professor, and A. D. PELTON, Professor, are both with Ecole Polytechnique (Université de Montréal), Box 6079, Station A, Montreal, Quebec, Canada, H3C 3A7.

Manuscript submitted June 9, 1982.

Analogously for g_B^E , one obtains:

$$g_B^E = \sum_{j=1}^M \phi_{m_j n_j} [n_j (1 - X_A)^{n_j - 1} + (1 - m_j - n_j) (1 - X_A)^{n_j}] X_A^{m_j} \quad [10]$$

In general, for the excess Gibbs energy of any constituent $A_x B_{1-x}$:

$$g_{A_x B_{1-x}}^E = \sum_{j=1}^M \phi_{m_j n_j} \{ (1 - m_j - n_j) X_A^{m_j} (1 - X_A)^{n_j} + [x m_j (1 - X_A) + (1 - x) n_j X_A] \cdot X_A^{m_j - 1} (1 - X_A)^{n_j - 1} - x^{m_j} (1 - x)^{n_j} \} \quad [11]$$

Setting $x = 1$ or $x = 0$ in Eq. [11] yields Eqs. [9] and [10], respectively.

Expressions analogous to Eqs. [9] to [11] can be written for the partial enthalpies of mixing Δh_A , Δh_B , and $\Delta h_{A_x B_{1-x}}$ and for the partial excess entropies of mixing s_A^E , s_B^E , and $s_{A_x B_{1-x}}^E$ in terms of the coefficients $h_{m_j n_j}$ and $s_{m_j n_j}$.

Hence, a set of coefficients $h_{m_j n_j}$ and a set of coefficients $s_{m_j n_j}$ are sufficient to express all thermodynamic properties of the solution provided that (i) polynomial expansions yield adequate representations of the excess properties, (ii) Δh and s^E are independent of T . These two conditions are met in practice by a large number of binary solutions. The present optimization technique seeks to obtain these two sets of coefficients from a critical self-consistent analysis of all the available diverse experimental thermodynamic and phase diagram data.

Although the present paper deals only with temperature independent polynomial expansions of Δh and s^E , in principle the optimization technique can be extended to expressions for Δh and s^E which are temperature dependent or which are other than simple polynomials.

II. THEORY

A. Basic Principles of Multiple Least Squares Regression Analysis with One Independent Variable

The least-squares method for calculating an expression which smoothly fits experimental data as closely as possible is one of the most popular techniques of regression analysis. Most computer installations have an "in-house" least-squares algorithm that is already programmed and can be "called" by any user of that computer. Since the theory and the computer algorithms are well documented elsewhere (for example, see References 8 to 10), only the basic principles will be presented here.

Suppose that for a dependent variable y and an independent variable x one has N experimental data point pairs y_i, x_i ($i = 1, N$). In order to fit these data via a least squares regression analysis to an equation, for example:

$$y = b_1 + b_2 x + b_3 x^2 + b_4 x \ln x \quad [12]$$

it is first necessary to set up a matrix z_{ij} , where:

$$\left. \begin{array}{l} z_{i1} = 1 \\ z_{i2} = x_i \\ z_{i3} = x_i^2 \\ z_{i4} = x_i \ln x_i \end{array} \right\} i = 1, N \quad [13]$$

The sum of the squares of the deviations is given by:

$$S = \sum_{i=1}^N \left(y_i - \sum_{j=1}^4 b_j z_{ij} \right)^2 \quad [14]$$

In the multiple least squares regression, S is minimized by setting $dS/db_j = 0$ for $j = 1, 4$. This yields 4 simultaneous linear equations which may be solved by a standard numerical method to obtain the coefficients b_j ($j = 1, 4$). One such method is the Gauss-Jordan reduction algorithm that is well documented in the literature. For example, an algorithm written in FORTRAN-IV is listed in Reference 10.

B. Least Squares Optimization of Binary Integral and Partial Gibbs Energies When T Is Constant

Suppose that at a constant temperature g^E has been measured at N_G different compositions, while g_A^E and g_B^E have been measured at N_{GA} and N_{GB} different compositions, respectively. One wishes to obtain a set of coefficients $\phi_{m_j n_j}$ ($j = 1, M$) in order to fit these data by least-squares regression to Eqs. [2], [9], and [10] simultaneously. This simultaneous fitting is made possible through the fact that Eqs. [2], [9], and [10] all are written in terms of the same coefficients $\phi_{m_j n_j}$. This is the crux of the present technique.

One first chooses the appropriate polynomial expansion (regular, sub-regular, etc.) by choosing M and by choosing the powers m_j and n_j . The independent variable is X_A . The total number of data points is $N = (N_G + N_{GA} + N_{GB})$. The dependent variable y_i and the matrix z_{ij} are then defined as follows:

$$y_i = g_i^E; \quad z_{ij} = X_A^{m_j} (1 - X_A)^{n_j} \quad \text{for } i = 1, N_G \quad [15]$$

$$y_i = g_{A_i}^E; \quad z_{ij} = [m_j X_A^{m_j - 1} + (1 - m_j - n_j) X_A^{m_j}] \cdot (1 - X_A)^{n_j} \quad \text{for } i = (N_G + 1), (N_G + N_{GA}) \quad [16]$$

$$y_i = g_{B_i}^E; \quad z_{ij} = [n_j (1 - X_A)^{n_j - 1} + (1 - m_j - n_j) \cdot (1 - X_A)^{n_j}] X_A^{m_j} \quad \text{for } i = (N_G + N_{GA} + 1), (N_G + N_{GA} + N_{GB}) \quad [17]$$

The sum of squares can now be written as in Eq. [14], and the coefficients $\phi_{m_j n_j}$ can be calculated.

If experimental data points for $g_{A_x B_{1-x}}^E$ of any constituent were available, these could be included in the analysis in a similar manner via Eq. [11].

Experimental partial and integral enthalpy or partial and integral excess entropy data could be fitted in an exactly analogous manner to find the coefficients $h_{m_j n_j}$ or $s_{m_j n_j}$.

In practice it is frequently desirable to "weight" certain experimental points more heavily than others. This may be accomplished by multiplying both y_i and z_{ij} for this point by a "weighting factor", w_i . If desired, this can be done in a systematic manner by "normalizing" such that $w_i y_i = 1$ for all i . The use of weighting factors will be discussed later in connection with the examples.

C. Least Squares Optimization of Binary Data in the General Case

In the general case, suppose that experimental data points g_i^E , $g_{A_i}^E$, etc. are available, each at a different T_i and X_{A_i} . By substituting Eq. [5] into Eqs. [2], [9], [10], and [11], one

can obtain all coefficients $h_{m_j n_j}$ and $s_{m_j n_j}$ simultaneously in a single regression analysis similar to that discussed above. Experimental enthalpy data, Δh_i , Δh_{A_i} , and Δh_{B_i} , can be treated in the same regression analysis as the Gibbs energy data by considering an enthalpy data point to be an excess Gibbs energy data point at $T = 0$.

Another source of thermodynamic data is an experimental miscibility gap, since the activities of each component are equal on the two phase boundaries at each end of a tie-line, even though the actual values of the activities may not be known. These data can also be treated simultaneously with all the other data as will be discussed later in connection with example 5.

An interactive computer program called FITBIN has been written to carry out the optimization analysis. This program simply applies the least-squares method (section II-A) to the Eqs. [15] to [17]. The user enters all the raw experimental data points (activities, enthalpies, temperature-composition coordinates of measured phase boundaries, etc.) and then interacts with the computer by changing weighting factors, changing the number of terms in the polynomial expansions and so on until, in his estimation, the "optimum" representation of the data has been obtained. Several examples of optimization analyses will now be presented.

III. SAMPLE CALCULATIONS

A. Example 1—Optimization of Isothermal Data for Partial Properties of Both Components

The partial enthalpies of mixing of both Bi and Sn in liquid Bi-Sn alloys at 725 K have been measured independently by solution calorimetry.¹¹ Average values for each composition are given in Table I.

One could now fit the experimental values for Δh_{Sn} by least-squares regression to an appropriate polynomial expansion in the mole fractions, and then calculate Δh_{Bi} via the Gibbs-Duhem relationship, or *vice versa*. Alternatively, one could calculate the integral enthalpy, $\Delta h = X_{Sn}\Delta h_{Sn} + X_{Bi}\Delta h_{Bi}$, at each composition and then fit these values by a least squares regression to a polynomial expansion as in Eq. [5]. However, none of these methods makes full use of all the available data. The optimization

Table I. Partial Enthalpies for Bi-Sn Alloys at 725 K (J mol⁻¹)

X_{Sn}	Experimental ¹¹		Calculated (Eqs. [19] and [20])	
	Δh_{Bi}	Δh_{Sn}	Δh_{Bi}	Δh_{Sn}
1.0	510	25	544	0
0.9	456	-13	452	4
0.8	338	46	368	21
0.7	238	113	289	46
0.6	209	151	218	84
0.5	100	159	155	138
0.4	75	272	100	201
0.3	63	305	59	280
0.2	38	351	25	377
0.1	63	519	8	485
0.0	-13	636	0	615

method as discussed in section II-B, on the other hand, fully utilizes all the available information.

The 22 data points of Table I were substituted into Eqs. [16] and [17] (with partial enthalpies in place of partial excess Gibbs energies), with 'A' = Bi, 'B' = Sn, $N_G = 0$, $N_{GA} = 11$, $N_{GB} = 11$. The coefficients $h_{m_j n_j}$ were then calculated. With the choice of $M = 2$ coefficients (sub-regular solution) the calculated optimized coefficients were: $h_{11} = 613.8$ J, $h_{12} = -68.6$ J. Hence:

$$\Delta h = 613.8X_{Bi}X_{Sn} - 68.6X_{Bi}X_{Sn}^2 \quad \text{J mol}^{-1} \quad [18]$$

$$\begin{aligned} \Delta h_{Bi} &= 613.8(1 + (-1)X_{Bi})X_{Sn} - 68.6(1 + (-2)X_{Bi})X_{Sn}^2 \\ &= 545.2X_{Sn}^2 + 137.2X_{Bi}X_{Sn}^2 \quad \text{J mol}^{-1} \quad [19] \end{aligned}$$

$$\begin{aligned} \Delta h_{Sn} &= 613.8(1 + (-1)X_{Sn})X_{Bi} - 68.6(2X_{Sn} + (-2)X_{Sn}^2)X_{Bi} \\ &= 613.8X_{Bi}^2 - 137.2X_{Bi}^2X_{Sn} \quad \text{J mol}^{-1} \quad [20] \end{aligned}$$

Values of Δh_{Bi} and Δh_{Sn} calculated from Eqs. [19] and [20] are also listed in Table I. When the calculations were repeated with $M = 3$ or $M = 4$ coefficients, no significant improvement of the representation was obtained.

B. Example 2—Coupled Thermodynamic/Phase Diagram Analysis of a Simple Eutectic System with Limited Solid Solubility

The phase diagram of the Cd-Pb system is shown in Figure 1. This is a simple eutectic system with limited solid solubility on the Pb-rich side and negligible solid solubility in the Cd-rich solutions. The liquidus and solidus have been measured several times with good agreement among the measurements (± 2 °C for the liquidus). The enthalpy of mixing of the liquid has also been determined and is known to ± 105 J. All the data for this system are reviewed in Reference 12.

Excess partial Gibbs energies of Cd and Pb can be calculated at points along their respective liquidus lines from the well-known expression:

$$RT \ln X_A^l + g_A^E - RT \ln a_A^s = -\Delta g_{f(A)}^o \quad [21]$$

where $A = \text{Cd or Pb}$, $T = \text{liquidus temperature}$, $X_A^l = \text{liquidus composition at } T$, $a_A^s = \text{activity with respect to pure solid } A \text{ in the solid on the solidus at } T$, and $\Delta g_{f(A)}^o$ is the molar Gibbs energy of fusion of A at T . For Cd, one can set $a_{Cd}^s = 1.0$ since there is negligible solid solubility. For Pb, one can assume that Raoult's Law holds in the dilute solid solutions such that $a_{Pb}^s = X_{Pb}^s$ where X_{Pb}^s is the solidus composition at T . Free energies of fusion are given by Reference 13.

$$\begin{aligned} \Delta g_{f(Cd)}^o &= 3941 + 37.024T + 6.079 \times 10^{-3}T^2 \\ &\quad - 7.401T \ln T \quad \text{J mol}^{-1} \quad [22] \end{aligned}$$

$$\begin{aligned} \Delta g_{f(Pb)}^o &= 1937 + 46.129T + 5.899 \times 10^{-3}T^2 \\ &\quad - 8.268T \ln T \quad \text{J mol}^{-1} \quad [23] \end{aligned}$$

The enthalpy of the liquid has been fitted¹² by least-squares regression to the following expression:

$$\begin{aligned} \Delta h &= X_{Cd}X_{Pb}(15564 - 21184X_{Pb} + 35731X_{Pb}^2 \\ &\quad - 31752X_{Pb}^3 + 11042X_{Pb}^4) \quad \text{J mol}^{-1} \quad [24] \end{aligned}$$

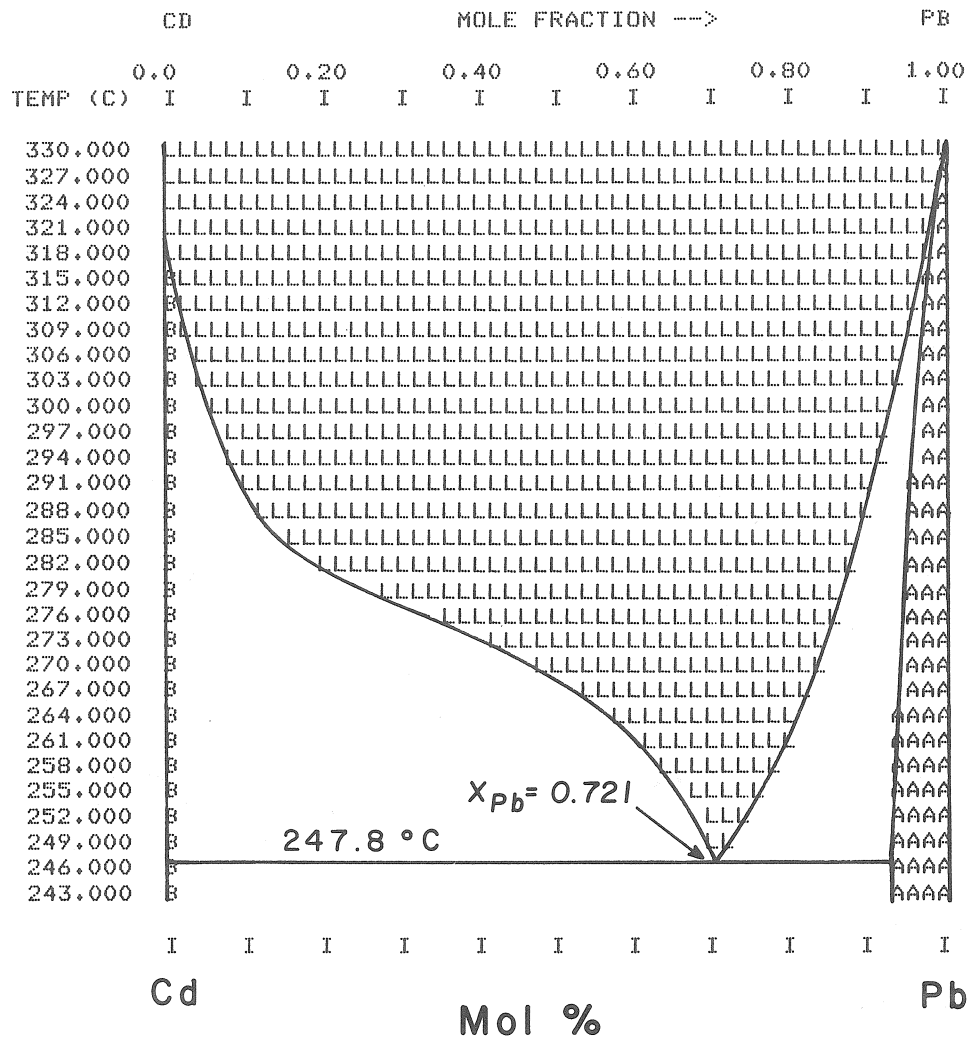


Fig. 1—Calculated Cd-Pb phase diagram.

By applying equations analogous to Eqs. [9] and [10], expressions for Δh_{Cd} and Δh_{Pb} can be calculated from Eq. [24].

At each experimental liquidus temperature and composition g_{Cd}^E or g_{Pb}^E can be calculated via Eq. [21]. By combining these values with the value of Δh_{Cd} or Δh_{Pb} at the same composition, one can calculate s_{Cd}^E at compositions between $X_{Cd} = 1$ and the eutectic composition $X_{Cd(E)}$, and one can calculate s_{Pb}^E at compositions between $X_{Pb} = 1$ and the eutectic composition.

Without access to the optimization technique, one would now be obliged to calculate s_{Pb}^E for $X_{Cd} > X_{Cd(E)}$ by applying the Gibbs-Duhem integration over this composition range with s_{Pb}^E at $X_{Cd(E)}$ used as end-point for the integration. Then one would calculate s_{Cd}^E for $X_{Cd} < X_{Cd(E)}$ by a similar operation. It would then be necessary to smooth these data in some manner to obtain a polynomial expansion for s^E . However, with the optimization technique one simply optimizes the two sets of partial excess entropy data together in exactly the same manner as was done with the partial enthalpy data in example 1.

These calculations are further greatly expedited by the program FITBIN. The user enters as input only the coeffi-

cients of Eq. [24] for Δh , the coefficients of Eqs. [22] and [23] for the free energies of fusion, and the T, X coordinates of the experimental liquidus and solidus points. He assigns weighting factors to each experimental point, and specifies the number M of the coefficients $s_{m/n}$ to be calculated. All other calculations (calculation of partial enthalpies, calculation of excess Gibbs energies from Eq. [21], calculation of partial excess entropies, and optimization) are then performed automatically.

From the calculated equations it is then possible to compute the binary phase diagram. In the present case this was done with aid of the F*A*C*T thermodynamic computer center.¹⁴ Figure 1 shows a computer-generated phase diagram. A tabular output of phase boundaries can also be generated so that precise comparisons can be made. If the fit is not satisfactory, the user can then go back and change the number of coefficients or the weighting factors, etc., until, in his estimation, the "optimum" fit has been obtained. This interactive conversation between user and computer permits a critical analysis of all the data to be carried out rapidly. Complete details of the operation of the programs are given in Reference 14.

With 5 entropy coefficients, the following optimized equation was obtained:

$$s^E = X_{Cd}X_{Pb}(6.569 - 20.435X_{Pb} + 50.999X_{Pb}^2 - 63.291X_{Pb}^3 + 30.0516X_{Pb}^4) \text{ J mol}^{-1}\text{K}^{-1} \quad [25]$$

Agreement between the calculated diagram and measured liquidus points is of the order of $\pm 1^\circ$. The calculated eutectic composition and temperature agree within $\pm 0.5^\circ$ and ± 0.3 mol pct with the various measurements. Details are given in Reference 12. Hence, the polynomial representation of thermodynamic properties is capable of reproducing the measured phase diagram within experimental error limits, even when the measurements are very precise.

In this example the experimental Δh data were first fitted to Eq. [24], and then the phase diagram data were used to optimize the expression for s^E . It would also have been possible to optimize the calorimetric Δh data and the phase diagram simultaneously. That is, in the input to the computer program one would give the experimental Δh , X data points and the T , X coordinates of the phase diagram. The coefficients h_{m_i} and s_{m_i} would then be optimized simultaneously by the technique of section II-C. In the present example, in which the data are very precise, either technique works well.

Partial Gibbs energies of Cd and Pb in the liquid calculated via Eqs. [9] and [10] agree within ± 125 J with values measured by emf and vapor pressure techniques (see Reference 12). Hence, the present analysis is in excellent agreement with the measured thermodynamic properties of the liquid. These liquid activity data could also have been included as input in the optimization procedure. In this case, the calculated functions for Δh and s^E would probably have been marginally more accurate, but the calculated phase diagram would not have agreed within $\pm 1^\circ$ with the measured diagram. Since all experimental data are never completely self-consistent, a decision as to which data one wishes to include in the optimization and which data one wishes to compare "after the fact" is inescapable.

Furthermore, the accuracies of the different data sets can vary greatly and the number of data points is rarely sufficient to constitute a statistical sample. Thus, no satisfactory objective statistical criterion can be applied to determine how many coefficients, M , give an "optimum" fit. This decision must always be made with an element of subjectivity.

In the optimization of the Cd-Pb system, weighting factors of 5 were applied to the experimental eutectic points. This choice was made on the basis of the fact that eutectic temperatures are usually known quite accurately. The choice of weighting factors is made on the basis of experience. Objective "normalization" techniques as discussed in section II-B rarely work well in practice.

C. Example 3—Coupled Thermodynamic/Phase Diagram Analysis with Intermediate Solid Compounds

The phase diagram of the PbCl_2 -KCl system is shown in Figure 2. Liquidus points have been measured (by Reference 15) to $\pm 3^\circ$. There are two intermediate solid compounds, $(\text{PbCl}_2)_{2/3}(\text{KCl})_{1/3}$, and $(\text{PbCl}_2)_{1/3}(\text{KCl})_{2/3}$. There is no evidence of solid solubility.

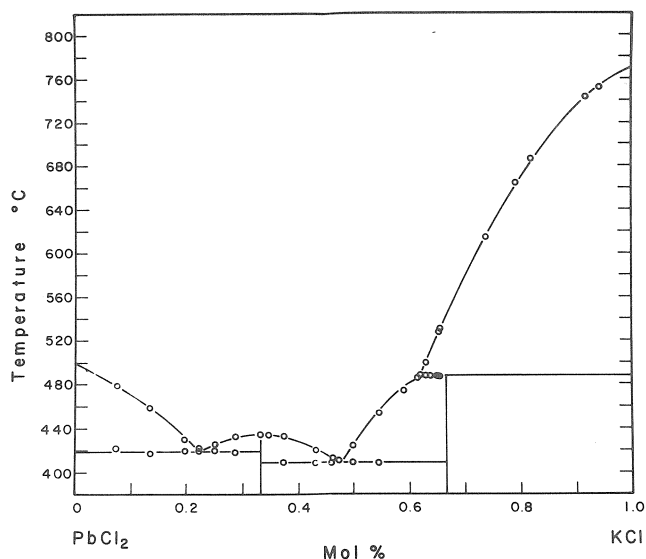


Fig. 2—Calculated (lines) and measured (points)¹⁵ phase diagram of the PbCl_2 -KCl system.

The experimental¹⁶ enthalpies of mixing in the liquid have been fitted¹⁵ to the following expression:

$$\Delta h = X_{\text{PbCl}_2}X_{\text{KCl}}(-17619 + 3004X_{\text{KCl}} - 28945X_{\text{KCl}}^2 + 15288X_{\text{KCl}}^3) \text{ J mol}^{-1} \quad [26]$$

From their known¹³ Gibbs energies of fusion, partial excess Gibbs energies of PbCl_2 and KCl can be calculated along their respective liquidus lines via Eq. [21]. If the Gibbs energies of fusion of the two intermediate compounds were also known (as is the case in some systems), then their partial excess Gibbs energies could also be calculated along their liquidus lines from Eq. [21], and an optimization analysis on all four partial properties could be carried out exactly as in example 2. In the present system, however, these Gibbs energies of fusion are not known. Hence, experimental liquidus points along only the PbCl_2 - and KCl-liquidus lines were used along with Eq. [26] for Δh in the optimization analysis, exactly as in example 2, to obtain the following expression for s^E :

$$s^E = X_{\text{PbCl}_2}X_{\text{KCl}}(6.159 + 2.130X_{\text{KCl}} - 15.016X_{\text{KCl}}^2) \text{ J mol}^{-1}\text{K}^{-1} \quad [27]$$

The function $s^E/X_{\text{PbCl}_2}X_{\text{KCl}}$ is well-behaved. Therefore, assuming that this expression interpolates well across the central composition region between the PbCl_2 - and KCl-liquidus lines, one can calculate $g_{(\text{PbCl}_2)_{2/3}(\text{KCl})_{1/3}}^E$ and $g_{(\text{PbCl}_2)_{1/3}(\text{KCl})_{2/3}}^E$ in this region from Eqs. [26] and [27] via Eq. [11]. One can then use Eq. [21] to calculate the Gibbs energies of fusion of the two compounds from their measured liquidus points. (All these calculations can be performed automatically by the computer. The user need enter as input only the T , X coordinates of the liquidus points.) The resultant expressions for the Gibbs energies of fusion were obtained¹⁵ as:

$$\Delta g_{f(\text{PbCl}_2)_{2/3}(\text{KCl})_{1/3}}^\circ = 19707 - 27.870T \text{ J mol}^{-1} \quad [28]$$

$$\Delta g_{f(\text{PbCl}_2)_{1/3}(\text{KCl})_{2/3}}^\circ = 11954 - 15.594T \text{ J mol}^{-1} \quad [29]$$

The phase diagram calculated from Eqs. [26] to [29] is shown in Figure 2. Agreement with the measured diagram is within the experimental error limits of $\pm 3^\circ$.

D. Example 4—Phase Diagram Analysis—Complete Liquid and Solid Solubility

The measured¹⁷ LiCl-FeCl₂ phase diagram is shown in Figure 3. No thermodynamic data for either phase are available. Under the assumption that the liquid is ideal ($g_{\text{LiCl}}^E = g_{\text{FeCl}_2}^E = 0$ in the liquid), Eq. [21] can be used along with the known Gibbs energies of fusion and the phase diagram to calculate the activities, a_{LiCl}^s and $a_{\text{FeCl}_2}^s$, along the solidus. Hence, the partial excess Gibbs energies in the solid, $g_{\text{LiCl}}^{E(s)}$ and $g_{\text{FeCl}_2}^{E(s)}$, along the solidus can be calculated. Under the assumption that $s^{E(s)} = 0$ in the solid, these partial properties were then optimized to obtain the following expression for the enthalpy of the solid:

$$\Delta h^s = 2100X'_{\text{LiCl}}X'_{\text{FeCl}_2} + 8611X'_{\text{LiCl}}X'^2_{\text{FeCl}_2} \quad \text{J/equivalent} \quad [30]$$

where Δh^s is the enthalpy of mixing per equivalent of solution (one mole LiCl = one equivalent, one mole FeCl₂ = 2 equivalents), and X'_{LiCl} and X'_{FeCl_2} are the equivalent fractions:

$$X'_{\text{LiCl}} = \frac{X_{\text{LiCl}}}{X_{\text{LiCl}} + 2X_{\text{FeCl}_2}} = 1 - X'_{\text{FeCl}_2} \quad [31]$$

In charge-asymmetric ionic solutions it is often desirable to use equivalent fractions rather than molar fractions in the polynomial expansions for the excess properties.

The phase diagram calculated under the assumptions of liquid ideality and $s^{E(s)} = 0$ with Eq. [30] for the enthalpy of the solid agrees with the measured diagram within the error limits of the latter.

In principle, it is possible to calculate both the enthalpy of the liquid, Δh^l , and the enthalpy of the solid, Δh^s , from the measured phase diagram alone if it is assumed that $s^E = 0$ in both phases. Hence, a simultaneous two-phase optimization could be carried out to obtain the coefficients $h_{m_j n_j}$ of both Δh^l and Δh^s in one operation. Equations to perform two-phase optimizations have been proposed by Lukas and co-workers.¹ In practice, such calculations are extremely sensitive to the curvatures of the measured liquidus and solidus,¹⁸ and experience has shown that measured phase diagrams are rarely of sufficient accuracy to permit meaningful results to be obtained.

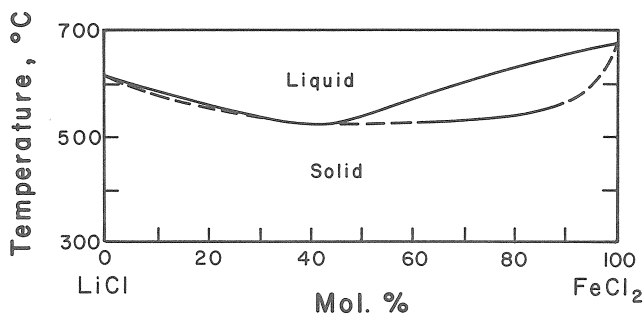


Fig. 3—Measured¹⁷ LiCl-FeCl₂ phase diagram (reproduced from Ref. 20).

E. Example 5—Phase Diagram Analysis—Regions of Immiscibility

A portion of the measured¹⁹ phase diagram of the Au-Ni system is shown in Figure 4. The system exhibits a region of immiscibility. Let $X_{\text{Au}(L)}$ and $X_{\text{Au}(R)}$ be the mole fractions of Au at the left and right ends of a tie-line. Equating the activity of Au at these two points, one obtains:

$$RT \ln X_{\text{Au}(L)} + g_{\text{Au}(L)}^E = RT \ln X_{\text{Au}(R)} + g_{\text{Au}(R)}^E \quad [32]$$

where the partial excess Gibbs energies at the left and right ends of the tie-line may be expressed by Eq. [9]. Substituting in Eq. [9] and rearranging yields:

$$RT \ln \frac{X_{\text{Au}(L)}}{X_{\text{Au}(R)}} = \sum_{j=1}^M \phi_{m_j n_j} \{ [n_j(1 - X_{\text{Au}(R)})^{n_j-1} + (1 - m_j - n_j) \cdot (1 - X_{\text{Au}(R)})^{n_j}] X_{\text{Au}(R)}^{m_j} - [n_j(1 - X_{\text{Au}(L)})^{n_j-1} + (1 - m_j - n_j)(1 - X_{\text{Au}(L)})^{n_j}] \cdot X_{\text{Au}(L)}^{m_j} \} \quad [33]$$

Experimental values of $X_{\text{Au}(L)}$ and $X_{\text{Au}(R)}$ can be optimized via Eq. [33] by the methods of section II, since the right-hand side of Eq. [33] is linear in the coefficients $\phi_{m_j n_j}$. That is, in the notation of section II, one sets:

$$y_i = RT_i \ln \frac{X_{\text{Au}(L)i}}{X_{\text{Au}(R)i}} \\ z_{ij} = [n_j(1 - X_{\text{Au}(R)i})^{n_j-1} + \dots X_{\text{Au}(L)i}^{m_j}] \quad [34]$$

where $X_{\text{Au}(L)i}$ and $X_{\text{Au}(R)i}$ are the experimental compositions at the ends of a tie-line at temperature T_i .

A similar expression to Eq. [33] can be written by equating activities of Ni at either end of each tie-line. Hence, each experimental tie-line results in two experimental "data points".

Enthalpies of mixing of the solid Au-Ni solution have been evaluated.¹⁹ These enthalpy data points as well as the T, X coordinates of the measured miscibility gap were optimized simultaneously to yield both $h_{m_j n_j}$ and $s_{m_j n_j}$ in one operation. The resultant optimized expressions are:

$$\Delta h = X_{\text{Au}}X_{\text{Ni}}(21.506 + 18.887X_{\text{Ni}} + 8.858X_{\text{Ni}}^2 - 22.121X_{\text{Ni}}^3) \quad \text{kJ mol}^{-1} \quad [35]$$

$$s^E = X_{\text{Au}}X_{\text{Ni}}(19.104 - 20.928X_{\text{Ni}} + 42.986X_{\text{Ni}}^2 - 35.095X_{\text{Ni}}^3) \quad \text{J mol}^{-1}\text{K}^{-1} \quad [36]$$

Equation [35] reproduces the measured enthalpy data within the experimental error of $\pm 125 \text{ J mol}^{-1}$. The miscibility gap calculated from Eqs. [35] and [36] is compared with that measured in Figure 4. Equation [36] agrees with s^E obtained¹⁹ by combining measured emf and calorimetric data to within $\pm 1.3 \text{ J mol}^{-1}\text{K}^{-1}$.

IV. CONCLUSIONS

A technique, based upon least-squares regression, has been developed which permits diverse sets of thermo-

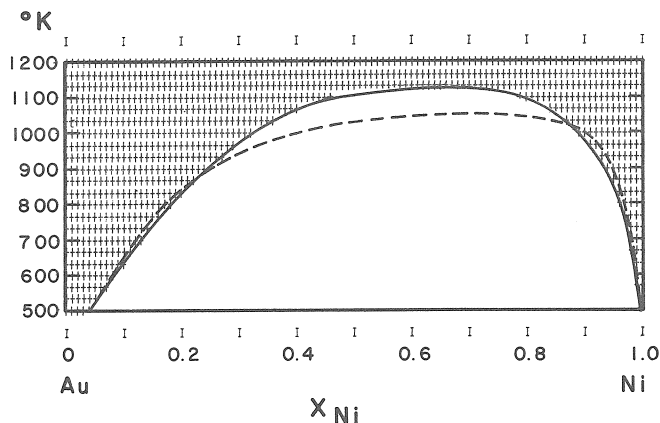


Fig. 4—Calculated ———, and measured¹⁹ - - - - -, solid-solid immiscibility gap in the Au-Ni system.

dynamic data for a binary phase (activities, enthalpies, etc.) as well as the binary phase diagram (which is also a source of thermodynamic data) to be simultaneously “optimized”. The results of this analysis are polynomial expansions for the enthalpy and excess entropy which give optimum fits to the thermodynamic/phase diagram data. As long as a polynomial expansion provides a reasonable representation of Δh and s^E , and as long as Δh and s^E may be assumed to be independent of temperature (as is the case in a great many systems), optimizations can be obtained which reproduce the experimental measurements well within their error limits. For example, phase diagrams calculated from the optimum equations can be accurate to better than 1°. Several examples of applications have been given. Phase boundaries involving intermediate binary compounds as well as immiscibility gap boundaries are included in the analyses.

An interactive computer program has been written to assist in this analysis. Experimental data points, such as the temperature-composition coordinates of phase boundaries, are read directly into the computer. The user can then interact with the program by changing weighting factors for the data points, by changing the number of coefficients in the polynomial expansions, and so on until, in his estimation, the “optimum” fit has been obtained. In this way, a critical analysis of a large number of diverse data can be rapidly carried out, and the resultant equations are self-consistent thermodynamically. These equations can be subsequently stored in computer data banks for calculation of any thermodynamic property or for calculation of the phase diagram. This program is available on-line to users of the F*A*C*T

(Facility for the Analysis of Chemical Thermodynamics) data bank and data treatment center.¹⁴

ACKNOWLEDGMENTS

Financial support in the form of a COOP grant and a Strategic grant from the Natural Sciences and Engineering Research Council of Canada is gratefully acknowledged.

REFERENCES

1. H. L. Lukas, E.-Th. Henig, and B. Zimmermann: *Calphad Journal*, 1977, vol. 1, p. 225.
2. P. Dörner, E.-Th. Henig, H. Krieg, H. L. Lucas, and G. Petzow: *Calphad Journal*, 1980, vol. 4, p. 241.
3. K. E. Spear and M. S. Wang: *Calphad Journal*, 1981, vol. 5, p. 109.
4. J. L. Haas, Jr. and J. R. Fisher: Proc. NBS Workshop on Application of Phase Diagrams in Metallurgy and Ceramics, National Bureau of Standards, Gaithersburg, MD, 1977, p. 909.
5. S. K. Tarby, C. J. Van Tyne, and M. L. Boyle: *ibid.*, p. 726.
6. N. Brouwer and H. A. J. Oonk: *Z. Phys. Chem. N. F.*, 1977, vol. 105, p. 113; *ibid.*, 1979, vol. 117, p. 55; *ibid.*, 1980, vol. 121, p. 131.
7. A. D. Pelton and C. W. Bale: *Calphad Journal*, 1977, vol. 1, p. 253.
8. M. L. Conneally and K. E. Fritz: “Computer Applications in Metallurgical Engineering”, R. D. Pehlke and M. J. Smith, eds., ASM, Metals Park, OH, 1963, chap. 8, p. 53.
9. J. Hilsenrath, G. G. Ziegler, C. G. Messina, P. J. Walsh, and R. J. Herbold: “OMNITAB-A Computer Program for Statistical and Numerical Analysis”, N. B. S. Handbook 101, U. S. Government Print. Office, Washington, DC, March 1966, p. 111.
10. B. Carnahan, H. A. Luther, and J. O. Wilkes: “Applied Numerical Methods”, J. Wiley and Sons Ltd., 1969, pp. 3, 571, and 282.
11. R. L. Sharkey and J. J. Pool: *Metall. Trans.*, 1972, vol. 3, p. 1774.
12. S. Ashtakala, A. D. Pelton, and C. W. Bale: *Bull. Alloy Phase Diagrams*, 1981, vol. 2, p. 83.
13. I. Barin, O. Knacke, and O. Kubaschewski: “Thermochemical Properties of Inorganic Substances” (and Supplement), Springer Verlag, Dusseldorf, 1973 (1977).
14. C. W. Bale, A. D. Pelton, and W. T. Thompson: “F*A*C*T—Facility for the Analysis of Chemical Thermodynamics”, User’s Guide and Supplement, Edition 1, McGill University/Ecole Polytechnique, Montréal, 1979.
15. A. Gabriel: Master’s Thesis, Department of Metallurgical Engineering, Ecole Polytechnique, Montréal, 1980.
16. F. G. McCarty and O. J. Kleppa: *J. Phys. Chem.*, 1964, vol. 68, p. 3846.
17. C. Beusman: U. S. Atomic Energy Comm., ORNL-2323, 20, 1957.
18. A. D. Pelton, H. Kohler, and A. Dubreuil: “Chemical Metallurgy—A tribute to Carl Wagner”, N. Gokcen, ed., American Institute of Metallurgical Engineers Conference Proceedings, New York, NY, 1981, pp. 273-82.
19. R. Hultgren, R. L. Orr, P. D. Anderson, and K. K. Kelley: “Selected Values of Thermodynamic Properties of Metals and Alloys”, Wiley, New York, NY, 1963.
20. E. M. Levin, C. R. Robbins, and H. F. McMurdie: “Phase Diagrams for Ceramists”, National Bureau of Standards, American Ceramic Soc. Inc., Fig. #1292, 1964.